

INTER-AMERICAN TROPICAL TUNA COMMISSION

SCIENTIFIC ADVISORY COMMITTEE

14th MEETING

La Jolla, California (USA)

15-19 May 2023

DOCUMENT SAC-14 INF-E

**LENGTH-STRUCTURED SPATIOTEMPORAL TAGGING MODEL FOR SKIPJACK IN
THE EPO**

Tobias K. Mildenberger, Anders Nielsen, Mark Maunder

CONTENTS

1. SUMMARY

Historically, assessing skipjack tuna (SKJ, *Katsuwonus pelamis*) in Eastern Pacific Ocean (EPO) has been problematic due to the lack of a reliable index of relative abundance, the possibility of a dome-shape selectivity, and the lack of age-composition data, challenging its sustainable management. A length-structured spatiotemporal population model allows estimation of movement as an advection-taxis-diffusion process and length-based mortality rates utilizing available tagging and effort data and might ultimately allow estimation of population size, distribution and sustainable harvest levels. While advection might be informed by ocean currents, taxis can be based on smooth habitat preference functions of environmental covariates such as sea surface temperature or the mixed layer depth. Movement rates and recapture probabilities can be estimated by means of the matrix exponential of instantaneous rates (Thorson et al., 2021) or the classic Kalman filter (Harvey, 1990). Results indicate that the movement of SKJ in the EPO is inversely related to the velocity of ocean currents and depends on sea surface temperature. SKJ prefers intermediate sea surface temperatures around 25-26°C and exhibits stronger undirected movement at low and high temperatures. Further, the model estimates length-based fishing mortality rates in space and time for each fleet and a length-based natural mortality rate in line with previously reported rates.

2. INTRODUCTION

The assessment of population dynamics and stock status is the foundation for the sustainable exploitation and effective management of marine resources. In the case of skipjack tuna (SKJ, *Katsuwonus pelamis*) in Eastern Pacific Ocean (EPO), the stock assessment has, historically, been problematic due to the lack of a reliable index of relative abundance, the possibility of a dome-shape gear selectivity, and the lack of age-composition data (Maunder, M.N. and Harley, S.J. 2005). At the same time, thousands of recaptures and tracks from conventional and archival tagging data are available and might serve as the basis for a spatiotemporal population model that allows estimating the abundance and exploitation rates of SKJ ([SAC-12-06](#)). In fact, the first implementation of the spatiotemporal tagging model ([SAC-13-08](#)) allowed estimation of movement rates based on environmental data and habitat suitability. Since then, the model has been developed further by implementing a faster algorithm to estimate fine-scale movement rates for a large spatial domain, incorporating archival tags and fishing effort data, including additional environmental variables, such as ocean currents, and accounting for the length of tagged fish. In this

report, we describe the updates since the first implementation of the spatio-temporal tagging model for SKJ in the EPO ([SAC-13-08](#)).

3. DATA

The required input data for the length-structured spatiotemporal tagging model are recovered and non-recovered conventional tags, archival tags, spatio-temporal effort data, as well as environmental data, such as information about ocean currents or sea water temperature.

3.1. Tagging data

Tagging data from four tagging events are available for SKJ in the EPO. In this study, we excluded data from the two oldest tagging events that took place before 1990 (1955-1964 and 1979-1981) but included tagging data from the two most recent events that took place from 2000 to 2006 and the ongoing event that started in 2019, as well as 30 tags that were released in 2011. While the six tuna tagging cruises in 2000 to 2006 targeted bigeye tuna, 3571 SKJ were tagged and released with plastic dart tags, of which 566 tags were recovered. The IATTC multi-year Regional Tuna Tagging Program (RTTP-EPO 2019-2022, Project E.4.a) that was initiated in 2019 focused on SKJ. The RTTP included three tagging cruises in 2019, 2020, and 2022. A total of 6431 SKJ were tagged with plastic dart tags during the cruises of which 1682 were recovered at the time of writing this report. A total of 9696 tag releases had sufficient and meaningful release information (e.g., speed < 200km/d), were released before 2022 and are considered for further analysis. Of all released tags, 2128 were recaptured before 2022 and had sufficient recapture information. 56 recaptured tags had to be excluded from further analysis as available information was not sufficient or unreliable. Besides 8 tag recaptures with insufficient information and one tag that was recaptured by a jig boat, all tags were recaptured by purse seiners and were assigned to the three set types (referred to as fleets in the remainder of this report), floating object associated sets (OBJ, 1209 tags), unassociated sets (NOA, 859 tags), and dolphin-associated sets (DEL, 64 tags). Although most tagged fish were released around the equator and 95°W, the recaptured fish span a wide region from 150°W to the coast of Peru and from 22°S to 20°N (Figure 1A).

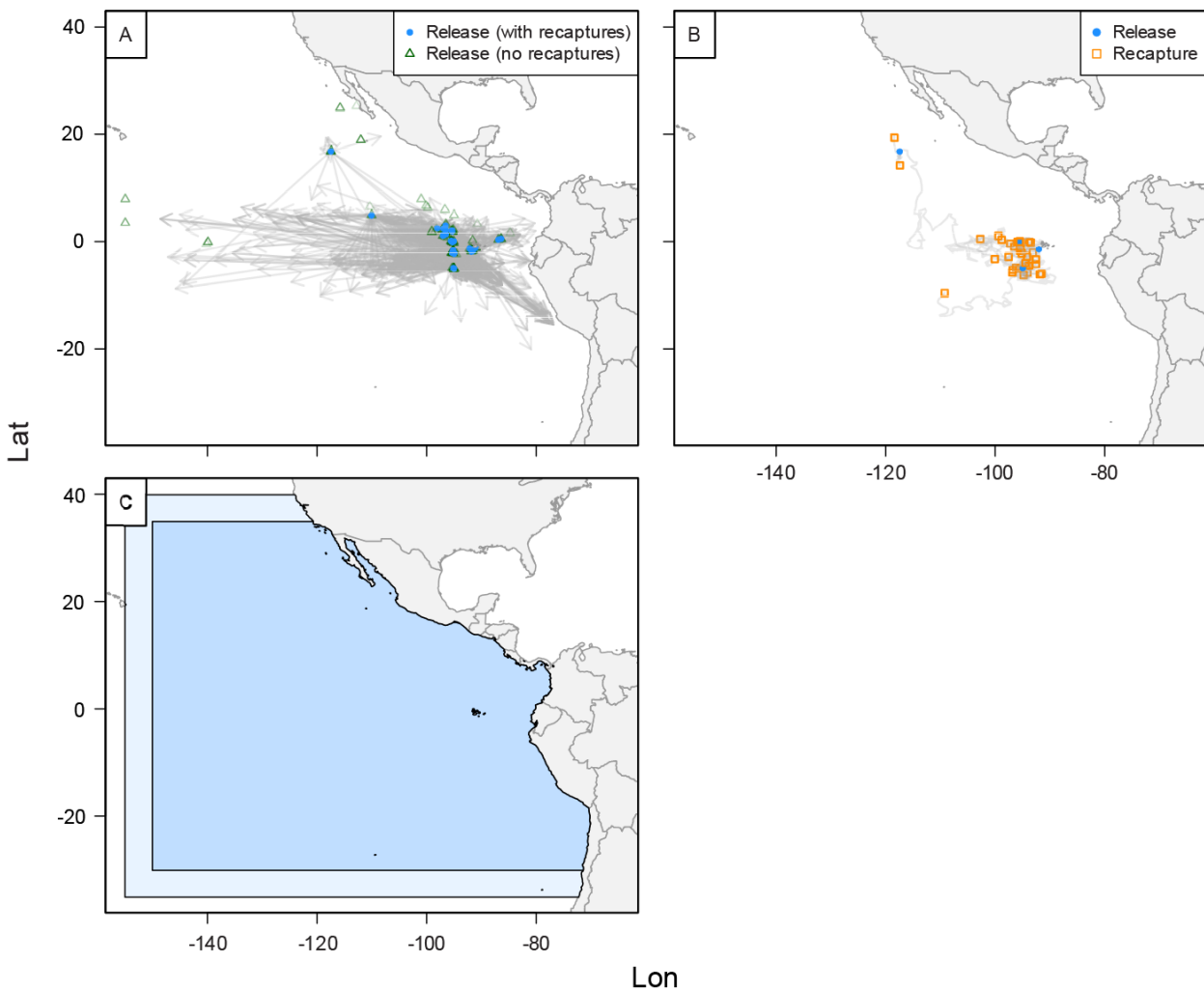


FIGURE 1. A) Release and recapture locations of the conventional tags from the 2000 and 2019 tagging programs. Release locations are indicated by a blue circle and recapture locations by arrow heads. B) Tracks of the 33 archival tags used in this analysis, where blue points indicate the release location and orange squares the recapture locations. C) Spatial domain of the EPO considered for the tagging and abundance model (dark blue), with a buffer 5° buffer zone (in light blue).

In addition to the conventional tags, 33 archival tags from the 2019-2022 RTTP were processed and used for the analysis (Figure 1B). Some archival tags that were recovered after 2021 or did not have sufficient information about the fleet that recovered the tag, or the length of the tagged fish were not considered in this analysis. The archival tags were recovered after 2 days to 8 months and travelled up to 15000 km. The most probable track was estimated with the unscented Kalman filter described in Lam et al. (2008). The spatial domain of the model was defined by the Western management boundary at 150°W and the coastline of North and South America in the East as well as the 30°S and 35°N (darker blue area in Figure 1C). An additional buffer zone of 5° around the model region was considered for the implementation of absorptive or reflective boundary conditions (lighter blue area in Figure 1C).

For 61% of the conventional tags the recapture location and date is known, due to on-board observers and having wells where the tags were found verified by tag recovery specialists. However, for the remaining 39% tags the exact well and/or set in which the tagged fish was recaptured is not known, and may have been from several wells and a number of different sets and these tags may have up to nine plausible recapture locations and dates (Figure 2A). While the majority of the possible recapture locations

are close to each other in time and space, the maximum range between possible recapture locations for a single tag spans several hundreds of kilometers and several weeks (Figure 2B-C).

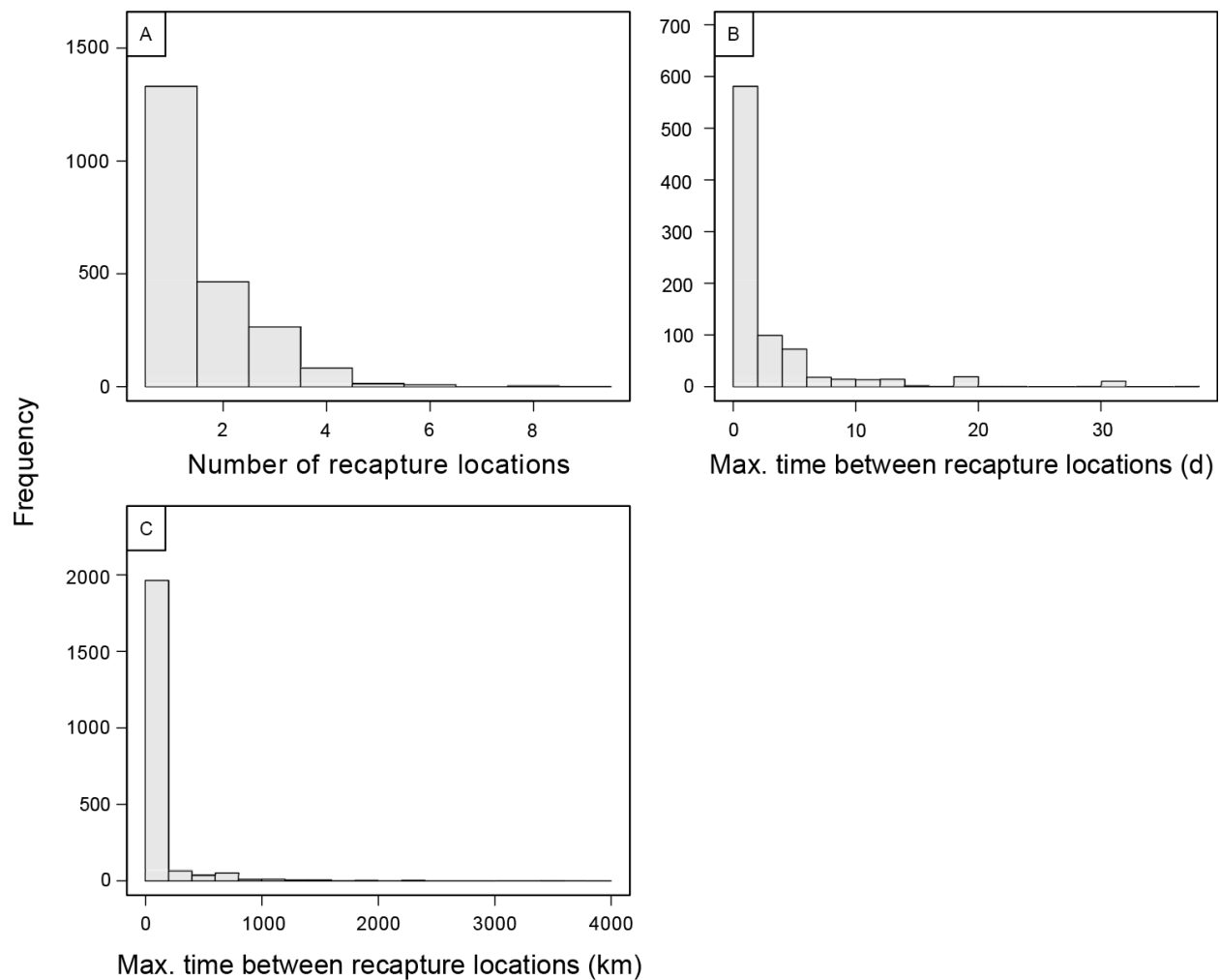


FIGURE 2: A) Number of tags with one or several recapture locations. B) Histogram of the maximum time in days between multiple recapture locations for a single tag. C) Histogram of the maximum distance in km between multiple recapture locations for a single tag.

A large proportion of tagged fish were recaptured within a short time after the release (even within the same day), these tags are not likely to contain a lot of information about the movement of the fish and might be affected by post-release stress. Thus, any tag that was recaptured within 14 days after the release, was removed from the analysis (280 tags). The length of all tagged fish is between 30 and 80 cm and shows a bimodal distribution with a peak around 48-50cm and around 65-70 cm (Figure 3).

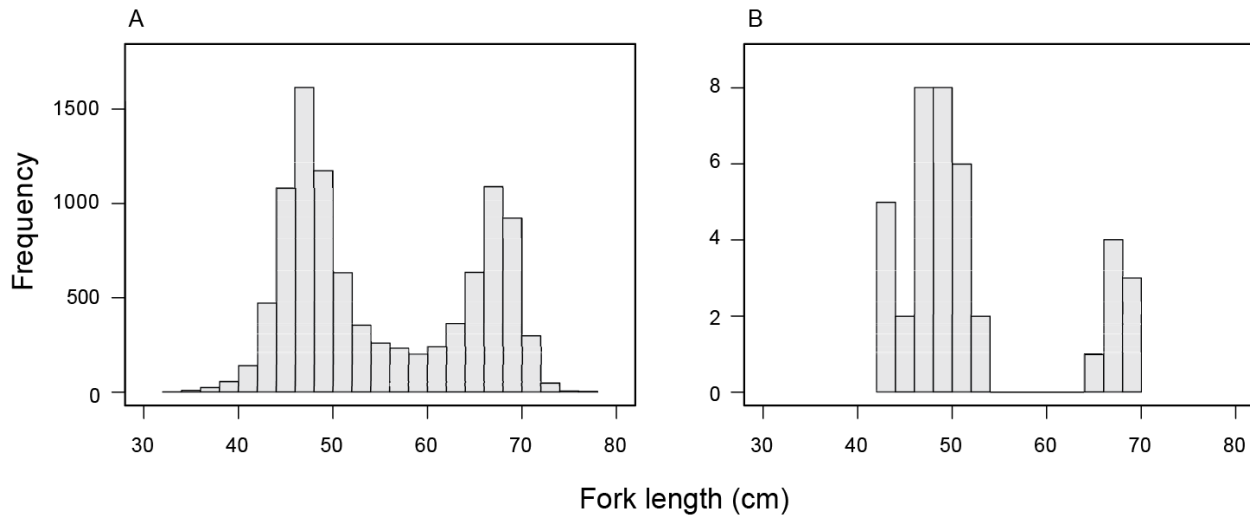


FIGURE 3: Fork length in cm at release of tagged fish for conventional tags (A) and archival tags (B).

3.2. Environmental data

The tagging model requires environmental data to inform the habitat preference of SKJ. A range of potential environmental covariates could be relevant for informing the habitat preference and thus movement of SKJ in the EPO. In this study, we used the ocean currents defined as the water velocity in meters per second (Figure 4) as covariates defining the advection and considered sea surface temperature in degree Celsius (SST; Figure 5), the mole concentration of dissolved molecular oxygen in sea water in the upper 10m (O_2 ; Supplementary Figure S1), and the mixed layer depth in meters (MLD; Supplementary Figure S2) as potential covariates informing the habitat preference and thus taxis of SKJ. The environmental data was aggregated to $2.5^\circ \times 2.5^\circ$ grid with monthly time steps for the period from 2000 to 2022.

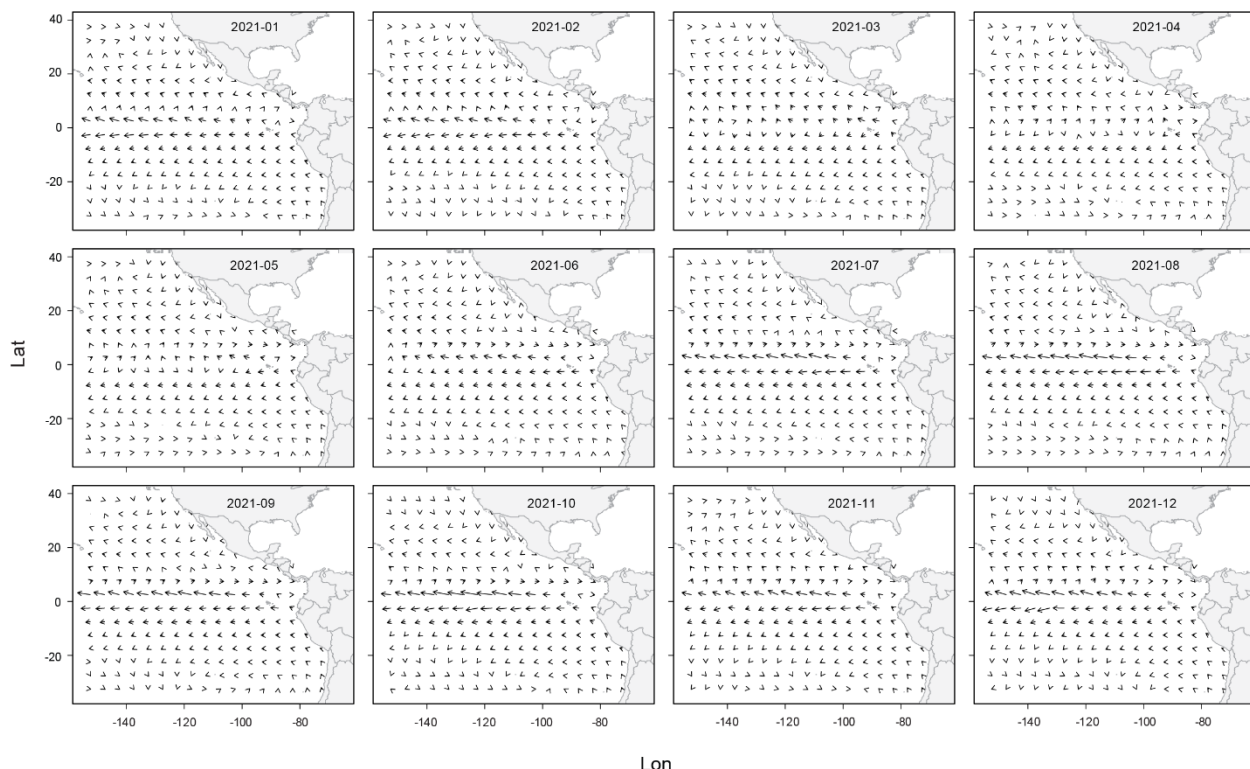


FIGURE 4: Average monthly velocity and direction of ocean currents in meters per second in 2021.

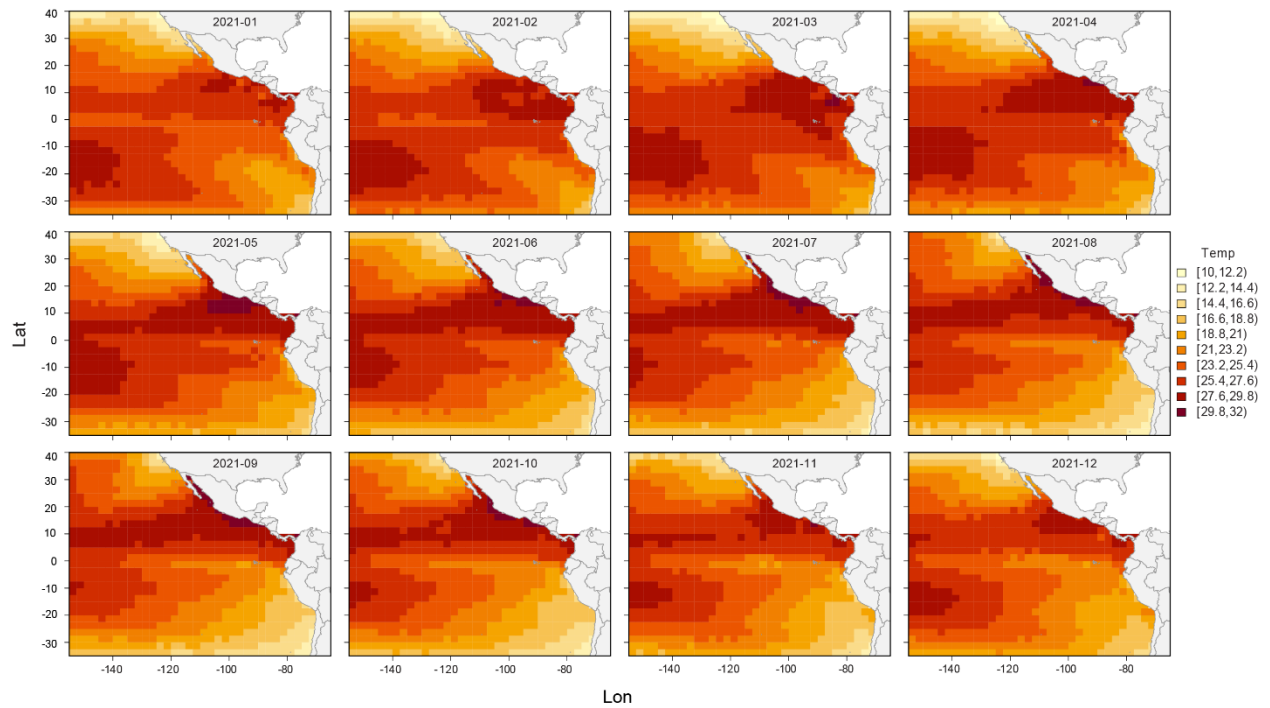
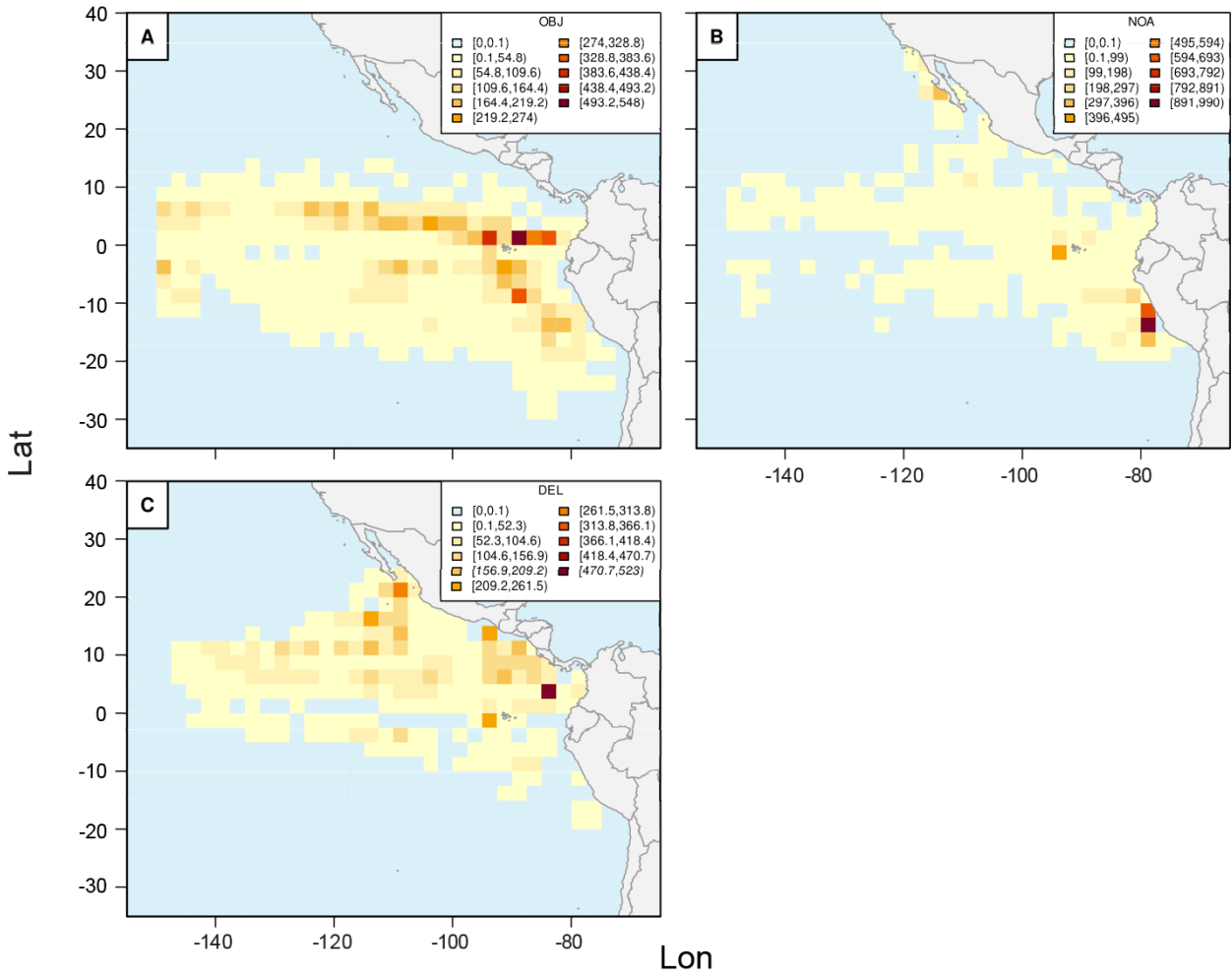
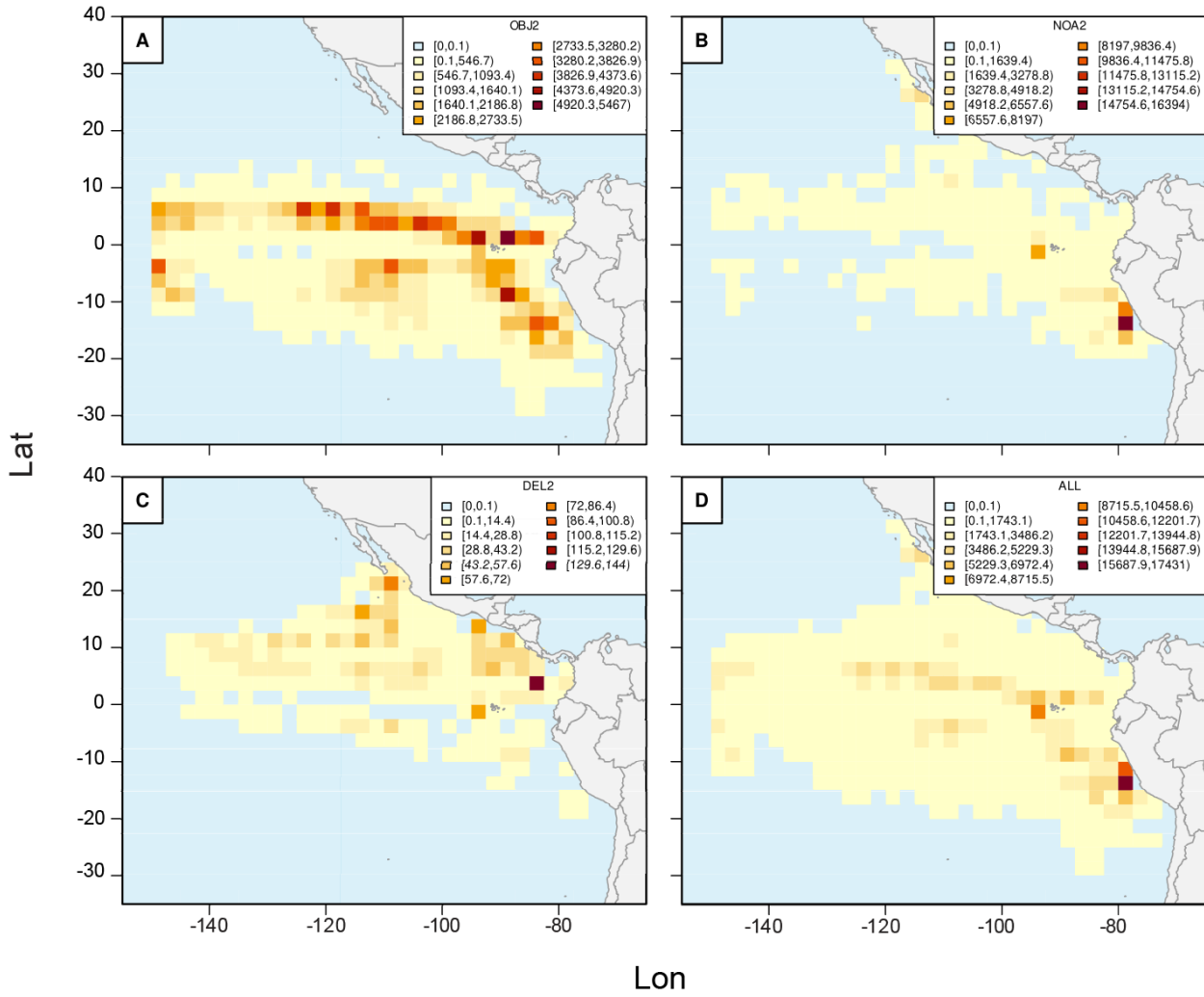


FIGURE 5: Average monthly sea surface water temperature in degree Celsius in 2021.

3.3. Effort data

Effort information of purse seiners was available from 2000 to 2021 as the number of sets on a fine spatial resolution ($1^\circ \times 1^\circ$ grid), per day, fleet (OBJ, NOA, DEL), and vessel size (class). The effort of the three purse seine fleets is not uniformly distributed throughout the model domain but shows higher levels north and south of the equator and close to the coastline and varies between fleets (Figure 6). This effort data contains important information about spatially varying recapture probabilities.





4. TAGGING MODEL

The tagging model consists of two components that describe the movement and natural and fishing mortality rates of SKJ in the EPO, respectively.

4.1. Movement

The movement is described by an advection-diffusion process that differentiates between undirected (diffusion) and directed movement informed by ocean currents (advection) and preferred habitat (taxis) as outlined by Thorson *et al.* (2021). Diffusion (D) can be assumed to be constant in space and time or be informed by smooth functions (natural spline) of any number of environmental fields. Advection (A) consists of an estimated scalar of the ocean currents in north-south and east-west direction. Taxis (T) is directed movement towards suitable habitat that is defined by the gradient of the preference function $h(g,t)$ that is the sum of smooth functions (s_i) with knots (k_i) and parameters (α_i) of any number of environmental fields (x_i).

$$h(g, t) = \sum_{i=1}^n s_i(x_i(g, t), k_i, \alpha_i)$$

Rather than the matrix exponential that was used in the first implementation ([SAC-13-08](#)), this implementation uses the classic Kalman filter for the definition of the model likelihood and the estimation of parameters (Harvey, 1990). While fast and memory efficient, this approach requires that the discrete environmental fields are differentiable over the whole spatial domain. This can be achieved by local interpolation where the locally interpolated field is defined in any position (*lon*, *lat*) by a weighted average of the input field values from a radius around the position. The distance-weighting of the local points is defined by an iterated cosine function to ensure differentiability (to a high enough order) when observation points are smoothly added or excluded from the average, as the position changes. If the radius is defined to be exactly equal to the distance between neighboring positions, then the value of the differentiable representation evaluated at an actual observation position will be exactly equal to the observed value (because exactly one observation is included), and at any other position the value will be a smooth weighted average of neighboring points. The advection field is defined as the gradient to the habitat field, and it is possible to evaluate the gradient of the local interpolation calculations. However, this gradient is zero if evaluated at the position of an observation and the radius is defined to be equal to the distance between neighboring points as then the calculation only involves taking the average of one point. To get useful gradient fields (one in the longitude direction and one in the latitude direction) the input fields for delta-longitude and delta-latitude were computed from each of the environmental fields and then the local interpolation method applied to get smooth versions. Hence each discrete environmental field x_i is converted into three smooth fields, that allow estimation of advection, taxis, and diffusion everywhere in the spatial domain in a differentiable way.

The observations $y_t = (\text{lon}_t, \text{lat}_t)$ of the archival tags at different times t between the time of release t_r and recapture t_R are assumed to be normally distributed around the true unobserved position ψ_t and observation noise Σ_y .

$$y_t \sim N(\psi_t, \Sigma_y)$$

$$\psi_{t+\Delta t} \sim N(\psi_t + A(\psi_t, t)\Delta t + T(\psi_t, t)\Delta t, 2D(\psi_t, t)\Delta t I_{2x2})$$

Where the unobserved true position at time $t+\Delta t$ depends on the previous position ψ_t and the sum of advection (A) and taxis (T). The diffusion (D) describes the standard deviation around the unobserved true position. While for recaptured conventional tags only the release and recapture positions are known, the likelihood of each recaptured conventional tag can be defined in the same way including several intermediate steps between the release and recapture time (here: daily time steps). The likelihood contribution of each conventional tag is then computed exactly as for the archival tags. Starting from the release location a Kalman filter is used to step from each timepoint and to the next (updating the distribution of the true unobserved position) and finally evaluating the likelihood of the recapture position. The only difference is that no observations are available at all the intermediate timesteps. The model assumes that movement rates are similar for all SKJ individuals, i.e., estimated movement rates do not depend on the size or age of the fish.

4.2. Mortality rates

The probability of the recovery of an archival or conventional tag at a given location and time does not only depend on the movement from the release to recapture location, but also the probability of the survival of the fish and the probability of capture at the recapture location by fleet f . We define the instantaneous fishing mortality $F_{p_m t_m l_m f}$ at location $p_m = (\text{lon}_m, \text{lat}_m)$ at time t_m and length l_m of fleet f

proportional to the effort of that fleet ($F_{p_m t_m l_m f} = \lambda_{l_m} E_{p_m t_m f}$), and the instantaneous natural mortality rate M_{l_m} at length l_m to be constant in space and time. That results in the following likelihood of recapture of the conventional tag i at time m .

$$\begin{aligned} L_i(M, \lambda | E) &= (1 - \Xi) (1 - \Omega) \frac{F_{p_m, t_m, l_m, f}}{M_{l_m} + \sum_{f=1}^F F_{p_m, t_m, l_m, f} + \omega} \\ &\quad (1 - e^{-(M_{l_m} + \sum_{f=1}^F F_{p_m, t_m, l_m, f} + \omega) \Delta t_m}) \\ &\quad \prod_{s=1}^{m-1} e^{-(M_{l_m} + \sum_{f=1}^F F_{p_s, t_s, l_m, f} + \omega) \Delta t_s} \end{aligned}$$

Where Ξ is the ratio of excluded recovered tags to all recovered tags accounting for excluding recovered tags with insufficient or unreliable information, Ω is the immediate shedding and non-reporting rate, ω is the continuous shedding rate, and the length of the fish at any time after the release time was estimated using the growth cessation model (Maunder et al. 2018) parameterized for SKJ in the EPO ([SAC-13-INF-J](#)). We set the immediate shedding and non-reporting rate to 0.45, and assume a continuous shedding rate of 0.0267 year⁻¹ as estimated by Hampton (2000). The length was categorized into length classes specified for the natural mortality and each fleet. We defined 12 length classes (30-40 cm and 3 cm bins for >40 cm) for natural mortality and the fishing mortality of the OBJ and 3 and 5 length classes for DEL and NOA, respectively, in the length-structured model. A larger number of length classes for DEL and NOA lead to more uncertain model parameters due to the lower number of recaptures for these two fleets. Setting Ξ , Ω , and ω to zero, the same likelihood can be used for the recapture of the archival tags.

A conventional tag that was not recovered, is either lost with the death of the fish due to natural causes, still attached to the living fish, was shed from the fish, or has been found but was not reported. Thus, the likelihood of the non-recaptured tag i can be defined as follows.

$$\begin{aligned}
L_i(M, \lambda | E) = & \Omega + (1 - \Xi)(1 - \Omega) \frac{M_{l_m}}{M_{l_m} + \sum_{f=1}^F F_{p_1, t_1, l_m, f} + \omega} \\
& (1 - e^{-(M_{l_m} + \sum_{f=1}^F F_{p_1, t_1, l_m, f} + \omega) \Delta t_1}) \\
& + (1 - \Xi)(1 - \Omega) \sum_{a=1}^A \frac{M_{l_m}}{M_{l_m} + \sum_{f=1}^F F_{p_a, t_a, l_m, f} + \omega} \\
& (1 - e^{-(M_{l_m} + \sum_{f=1}^F F_{p_a, t_a, l_m, f} + \omega) \Delta t_a}) \\
& \prod_{s=1}^{a-1} e^{-(M_{l_m} + \sum_{f=1}^F F_{p_s, t_s, l_m, f} + \omega) \Delta t_s} \\
& + (1 - \Xi)(1 - \Omega) \prod_{a=1}^A e^{-(M_{l_m} + \sum_{f=1}^F F_{p_a, t_a, l_m, f} + \omega) \Delta t_a}
\end{aligned}$$

Where A is the assumed maximum age of the fish (here: 5 years). Similar as to the environmental fields, the Kalman filter requires that effort is defined in a continuous differentiable way throughout the spatial domain of the model. Therefore, we used the local interpolation approach described above for the interpolation of the effort. The framework is optimized for computation speed and memory by grouping tags with various recovery locations and times but the similar release locations and times and implemented as a software package using the Template Model Builder (TMB; Kristensen *et al.* 2016) and R 4.0.2 (R Core Team 2020).

5. RESULTS

The length-structured spatio-temporal tagging model is able to estimate movement informed by ocean currents and sea surface temperature and length-based mortality rates based on spatial effort information. SST was the most robust environmental field for taxis and showed a similar preference function with a preferred temperature window around 25°C across a wide range of assumptions and scenarios. The preference function of O₂ and MLD and resulting taxis, on the other hand, was less robust and dependent on model settings. Thus, the following results focus on the use of SST for taxis.

In comparison to the simple model without length or effort information ([SAC-13-08](#); Figure 8A-C), including effort data into the model and thus accounting for the survival rates and recapture probability, changes the estimated preference function and habitat suitability (Figure 8D-F). While the preferred temperature window is for both models around 25°C, the absolute scale and shape of the preference function changes. For temperatures below the optimum, the model without effort predicts higher preference than the model that accounts for fishing effort (Figure 8A&D). Accounting additionally for the length of the fish results in a similar preference function to the effort model, but predicts higher preference for temperatures greater than 25°C (Figure 8G-I).

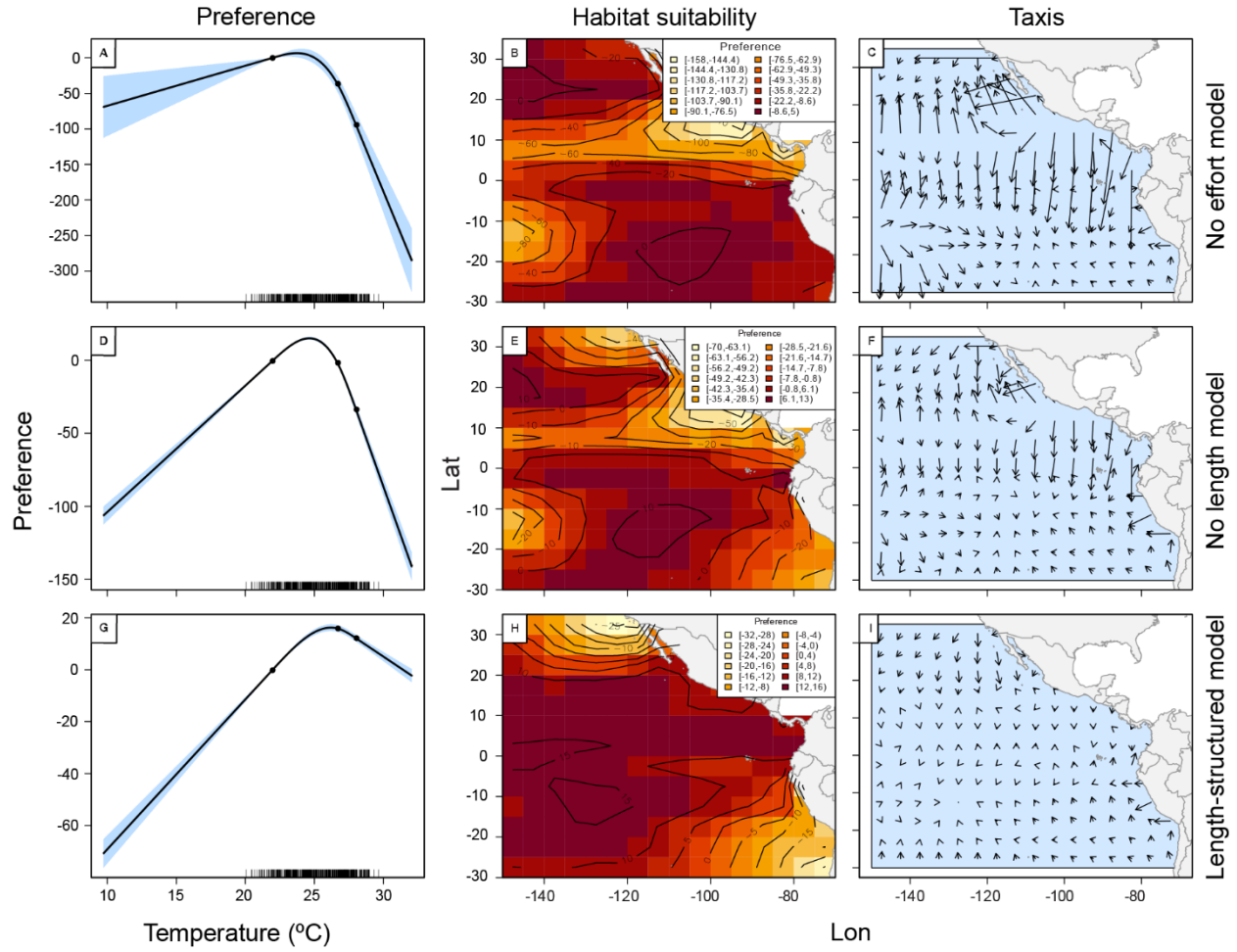


FIGURE 8: Preference function, habitat suitability, and taxis for the three models without effort data, without length structure, and the fully length-structured tagging model (rows).

Besides the effect on estimated movement, including effort information also allows us to estimate length-based natural and fishing mortality rates for each fishing fleet. Estimated natural mortality of the effort model without length information is around 2.75 year^{-1} and in line with estimated length-based values of the length structured model (Figure 9A). The length-based natural mortality rate suggests a variable pattern with larger values between $2-4.5 \text{ year}^{-1}$ for fish between 30-40 cm and above 58 cm and smaller values around $1.5-2.5 \text{ year}^{-1}$ for fish between 40-58 cm. The average fishing mortality over all years estimated by the effort model without length information is around 0.06 for DEL, 0.18 for NOA, and 0.36 year^{-1} for OBJ which corresponds well to the length-based estimates of the length-structured model (Figure 9B). However, the length-structured model suggests higher fishing mortality values for DEL and NOA for larger length classes ($>60\text{cm}$) similar in scale to the values of OBJ. OBJ on the other hand, shows high values above 0.4 year^{-1} for fish of 40-48 cm and 65-68 cm. The fishing mortality over time shows a similar pattern for the two models with high and variable rates for OBJ and lower and decreasing rates for NOA and DEL (Figures 9C&D). Estimated uncertainty is larger for the average fishing mortality rates over all length classes of the length-structured model.

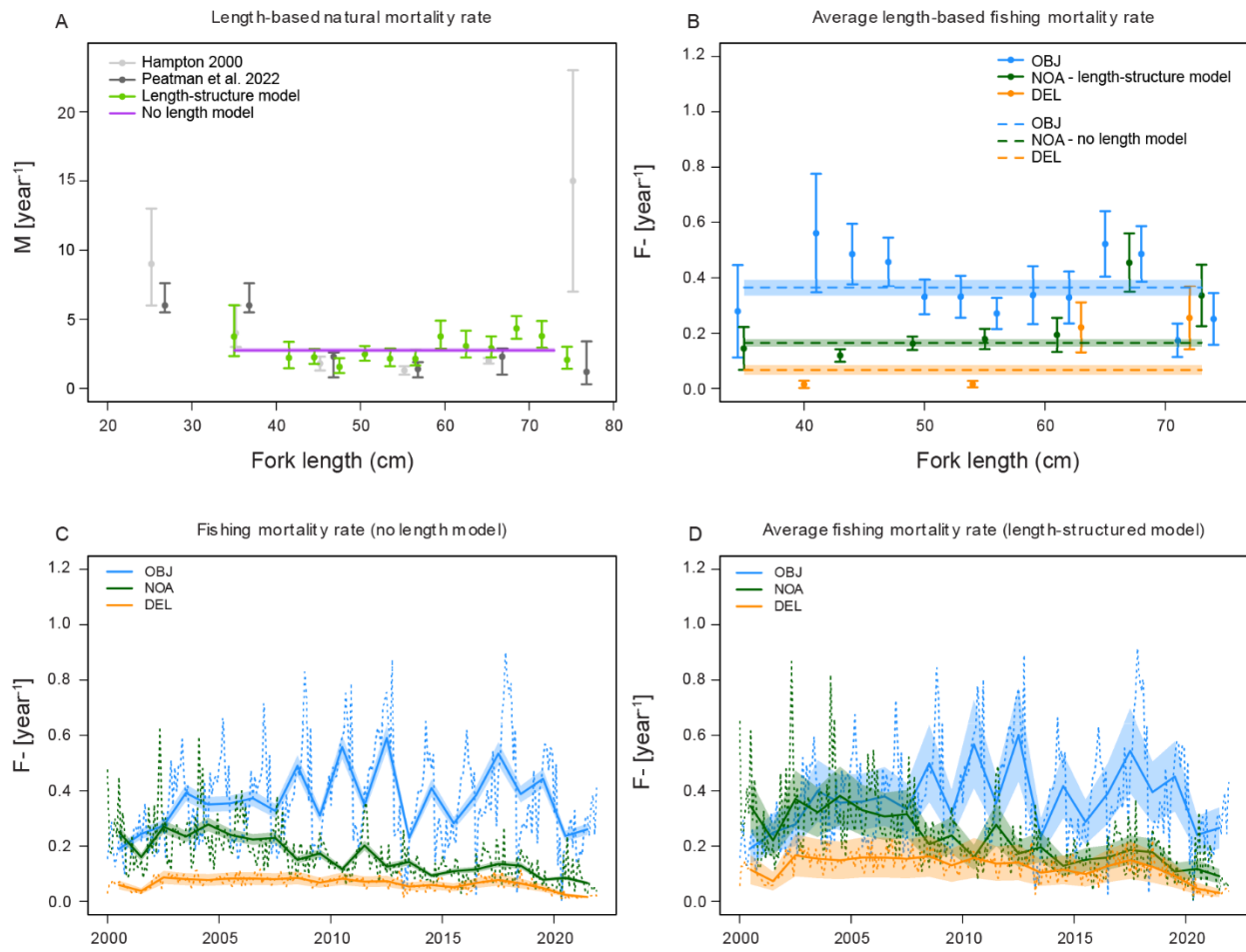


FIGURE 9: A) Length-based natural mortality rates. B) Length-based fishing mortality rates. C) Fishing mortality rates over time for the model without length. D) Average fishing mortality rate over all length classes of the length-structured model.

In addition to directed movement due to preferred temperature and taxis, the tagging model allows inclusion of directed movement based on the velocity of ocean currents. The overall model parameters and estimated movement patterns are not largely affected by the inclusion of the additional advection component (Supplementary Figure S4). However, interestingly, the estimated parameter relating advection to the ocean currents is negative (-1.7) implying that the advection component would be directed in the opposite direction to the currents.

Incorporating the information about the recapture uncertainty of conventional tags enables the tagging model to estimate an additional parameter specifying the uncertainty of the recapture locations. The estimated standard deviation is around 4.5 and leads to a lower estimated diffusion rate in comparison to a model without recapture location uncertainty information (Table 1).

TABLE 1: Estimated diffusion and tag uncertainty parameters for the model without and with recapture uncertainty. SD is the standard deviation.

Model	Parameter	Estimate	95% CI
Without recapture uncertainty	Diffusion	4.2	4.2 - 4.3
With recapture uncertainty	Diffusion	3.3	3.2 - 3.4
Estimate SD	SD(recapture location)	4.1	4.0 - 4.3

Diffusion can either be estimated to be constant in time and space or dependent on the environmental fields. A model with a variable diffusion rate depending on SST using a natural spline with two or three knots predicts higher diffusion with lower temperatures (2 and 3 knot model) and slightly higher diffusion with temperatures above 28°C (three-knot model) (Figure 10). Estimating variable diffusion as a smooth function of SST does not affect estimated taxis (Supplementary Figure S5) or mortality rates.

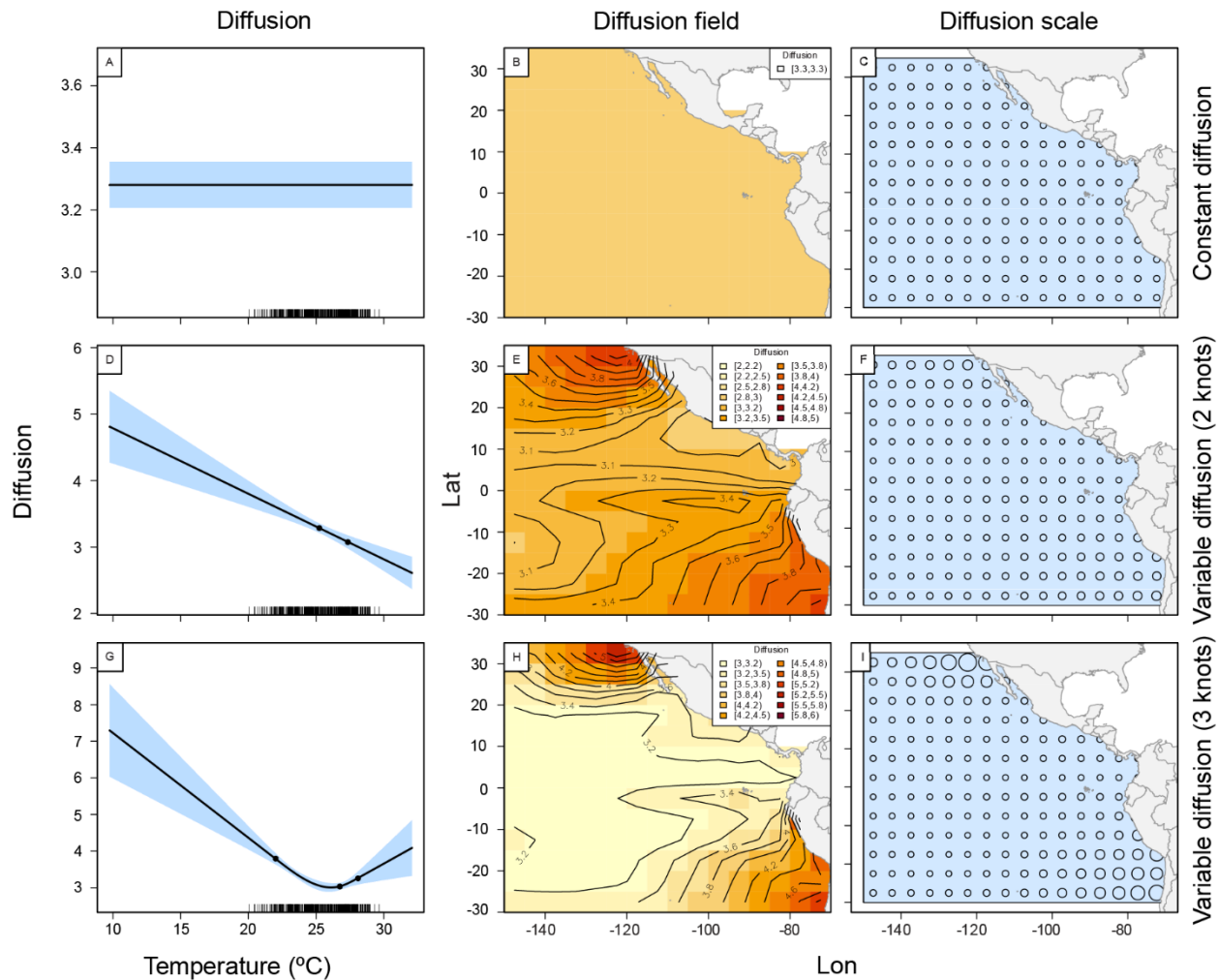


FIGURE 10: Preference function, habitat suitability, and diffusion (columns) for three models assuming constant diffusion (first row), temperature-dependent diffusion with two (second row) and three knots (third row).

Using the alternative effort expressed as the weighted sum of the number of sets accounting for the vessel size rather than the raw effort data does not affect estimated natural mortality rates but leads to slightly larger fishing mortality rates for NOA and DEL and a lower rate for OBJ (Figure 11A-F). Combining the

effort of all fleets corresponds to sum of the fishing mortality rates of the model with the weighted effort data and reveals an overall declining fishing mortality rate over the whole time series (Figure 11G-I). The estimated natural mortality rate is similar to the models with fleet-specific effort information.

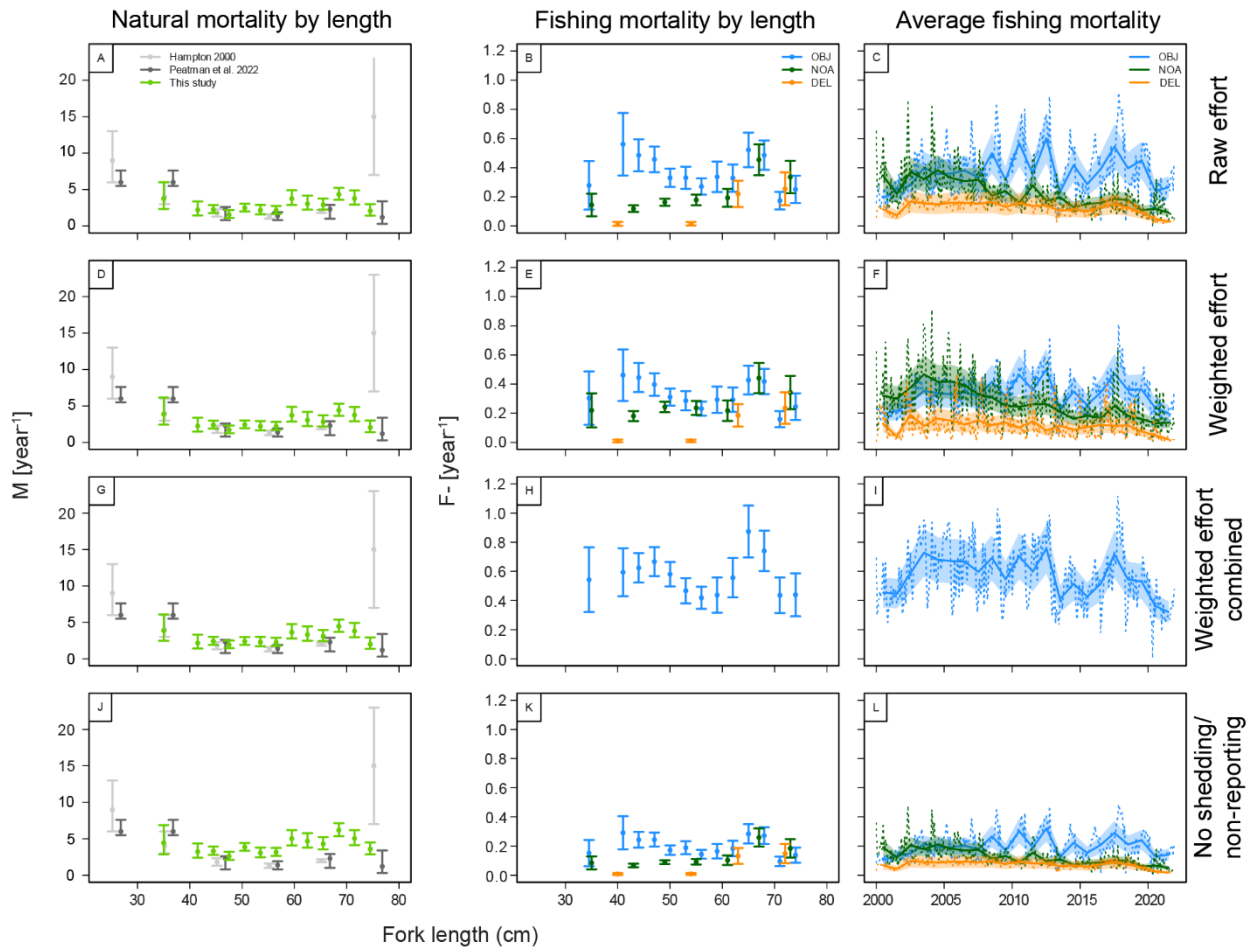


FIGURE 11: Natural mortality by length (first column), fishing mortality by length (second column), and fishing mortality over time (third column) for four models using the raw fishing effort (first row), using the catch rate weighted effort (second row), using the catch rate weighted effort combined for all fleets (third row), and assuming no tag loss (fourth row).

The assumed immediate and continuous tag loss rates due to shedding and non-reporting affect estimated mortality rates substantially. Assuming no tag loss increases natural mortality rates and decreases fishing mortality rates (Figure 11J-L).

6. DISCUSSION

Estimated movement patterns presented here are in line with the results of previous model implementations using the matrix exponential approach ([SAC-13-08](#)). The results show that ocean currents as well as SST are likely to be important drivers of the habitat suitability and movement of SKJ in the EPO. Variable diffusion dependent on SST can be estimated and mirrors the preference function suggesting a lower diffusion rate at the preferred habitat and higher diffusion outside the preferred habitat. The results of this analysis revealed that fine-scale spatial effort information and length-dependent mortality rates affect the estimated movement patterns. This can likely be attributed to the biased simplification of assuming uniformly distributed tag recapture probabilities in space and time as well as varying natural and fishing mortality rates for fish of various sizes. In terms of absolute scale, estimated (length-based) natural mortality rates are in line with values reported for SKJ in the eastern

(Hampton 2000) and central and western Pacific Ocean (Peatmann *et al.* 2022) (Figure 9&11). But also, the relative pattern by length of the length-structured model corresponds well to the literature values suggesting larger mortality for smaller and larger fish. At the same, estimated values for large fish >71cm are smaller than the high estimate of around 15 year⁻¹ by Hampton (2000) and more in line with Peatmann *et al.* (2022). Estimated length-based fishing mortality values underlines the importance of accounting for the length of the individuals as estimates for the two fleets NOA and DEL vary substantially between smaller and larger fish. The mortality rates can be estimated for fine length intervals if the data suffices as for example for OBJ. While natural mortality is relatively robust across a range of assumptions, fishing mortality rates depend on the definition and aggregation of the effort and the tag loss rates. As previously described (SAC-12-06), the raw effort of purse seiners measured as the number of sets per set type is problematic as it does not account for differences in vessel sizes, is not species-specific for SKJ, and does not (or it is not possible) include search time, and might thus not be directly proportional to fishing mortality as assumed in this analysis. An approach to account for the vessel size is to weight the number of sets per fleet (OBJ, NOA, DEL) by their catch rate. While this does not affect the natural mortality estimates considerably, estimated fishing mortality rates change substantially (Figure 11). The estimation of mortality rates as demonstrated here is relatively robust to the exclusion of conventional tags recovered within 7-30 days after the release (Supplementary Figure S6). While natural mortality at length and overall average fishing mortality over time are comparable between the different scenarios, the estimated average fishing mortality at length is greater for smaller individuals and lower for larger individuals when excluding tags recovered within 30 days in comparison to 7 days.

7. NEXT STEPS

The current length-structured spatio-temporal tagging model implementation relies heavily on the adequacy and assumptions of the effort data (Figure 8&11). While for other stocks and fisheries, adequate species-specific effort information might be available, for SKJ in the EPO, effort data defined as the number of sets (weighted by vessel size) might not be directly proportional to the fishing mortality rate. For this reason, future work will explore more flexible relationships between fishing mortality and effort, such as defining F as a smooth function of the effort field $F_{p_m t_m l_m f} = \lambda_{l_m} s(E_{p_m t_m f})$ or adding additional covariates (e.g., *lon* and *lat* fields) to the spatial effort data. While traditional length-structured versions of the Brownie-Peterson models (e.g., Fu, 2022; Hillary and Eveson, 2015; Peatmann *et al.*, 2022) allow to estimate stock abundance and exploitation rates independent of effort data, any spatial implementation of the Brownie-Peterson model either requires total mixing, spatial effort information, or assumes uniformly distributed effort in space and time, which is likely to be a coarse oversimplification given the spatial distribution of effort (Figure 6&7) and temporal trends (Supplementary Figure S3). The Brownie-Peterson model that does not account for spatially varying and length-dependent recovery probabilities likely leads to biased estimated movement patterns (as indicated by the scale and direction of the arrows in Figure 8C in comparison to Figure 8F&I) and requires to make specific mixing assumptions of tagged individuals with the untagged population. However, inclusion of spatial catch data along with a spatiotemporal model of abundance may provide a means to estimate spatial fishing mortality rates, which can be used to predict the tag recoveries. Future work should also investigate a parameterized function for the natural mortality by length by assuming e.g., the Gislason *et al.* (2010) or Lorenzen *et al.* (2022) function and only estimating the scale of the function as well as the fishing mortality assuming a parameterized function for the capture probability at length (selectivity curve) for each fleet. Furthermore, the estimation of seasonally varying movement rates and mortality parameters should be considered. For example, the movement according to currents and the probability of capture at length might vary seasonally. The analysis presented here also showed the importance and effect of immediate and continuous shedding and non-reporting rates on the model parameters and exploitation rates. It could be explored if these rates can be estimated inside the tagging model. Alternatively, they can be estimated outside of the model using available information from tag seeding and double-tagging experiments to derive up-to-date and stock-specific values. Ultimately, the goal of this model is to be able

to be used as a standalone length-structured assessment model to estimate stock abundance, exploitation rates, and biological reference points for sustainable exploitation, or to provide useful input to the interim assessment model (SAC-13-07). The next steps also include the development of model diagnostics and further sensitivity testing of the estimation of movement and mortality rates.

7. ACKNOWLEDGMENTS

This work was funded by IATTC and the European Union through grant agreement SI2.804586. We are grateful for comments on the methodology and data processing by Kurt Schaefer, Dan Fuller, Mitchell Lovell, Michael Opiekun, Kasper Kristensen, and Jon Lopez. We acknowledge the work done by COPERNICUS (<https://www.copernicus.eu/en>) and everyone involved in the tagging and recovery of SKJ tags in the EPO.

8. REFERENCES

- Fu, D., 2022. A length-based extension to the Brownie-Peterson model and its performance. *Fisheries Research*, 249, p.106248.
- Hampton, J., 2000. Natural mortality rates in tropical tunas: size really does matter. *Canadian Journal of Fisheries and Aquatic Sciences*, 57(5), pp.1002-1010.
- Harvey, A.C. (1990). Forecasting, structural time series models and the Kalman filter.
- Hillary, R.M. and Eveson, J.P., 2015. Length-based Brownie mark-recapture models: Derivation and application to Indian Ocean skipjack tuna. *Fisheries Research*, 163, pp.141-151.
- Gislason, H., Daan, N., Rice, J.C. and Pope, J.G., 2010. Size, growth, temperature and the natural mortality of marine fish. *Fish and Fisheries*, 11(2), pp.149-158.
- Kristensen, K., Nielsen, A., Berg, C.W., Skaug, H., Bradley M. and Bell, B.M. 2016. TMB: Automatic Differentiation and Laplace Approximation. *Journal of Statistical Software*, 70(5), 1-21. doi:10.18637/jss.v070.i05
- Lam, C. H., Nielsen, A., & Sibert, J. R. (2008). Improving light and temperature based geolocation by unscented Kalman filtering. *Fisheries Research*, 91(1), 15-25.
- Lorenzen, K., Camp, E.V. and Garlock, T.M., 2022. Natural mortality and body size in fish populations. *Fisheries Research*, 252, p.106327.
- Maunder, M.N. and Harley, S.J. 2005. Status of skipjack tuna in the eastern Pacific Ocean in 2003 and outlook for 2004. *Inter-Amer. Trop. Tuna Comm., Stock Assess. Rep.* 5: 109-167.
- Maunder, M.N., Deriso, R.B., Schaefer, K.M., Fuller, D.W., Aires-da-Silva, A.M., Minte-Vera, C.V. and Campana, S.E., 2018. The growth cessation model: a growth model for species showing a near cessation in growth with application to bigeye tuna (*Thunnus obesus*). *Marine Biology*, 165, pp.1-9.
- Peatman, T., Vincent, M.T., Phillips, J.S. and Nicol, S., 2022. Times are changing, but has natural mortality? Estimation of mortality rates for tropical tunas in the western and central Pacific Ocean. *Fisheries Research*, 256, p.106463.
- R Core Team (2020). R: A language and environment for statistical computing. R Foundation for Statistical Computing, Vienna, Austria. URL <https://www.R-project.org/>.
- Thorson, J.T., Jannot, J., and Somers, K., 2017. Using spatio-temporal models of population growth and movement to monitor overlap between human impacts and fish populations. *Journal of Applied Ecology*, 54(2), 577-587.

Thorson, J.T., Barbeaux, S.J., Goethel, D.R., Kearney, K.A., Laman, E.A., Nielsen, J.K., Siskey, M.R., Siwickie, K. and Thompson, G.G., 2021. Estimating fine-scale movement rates and habitat preferences using multiple data sources. *Fish and Fisheries*, 22(6), pp.1359-1376.

9. SUPPLEMENTARY MATERIAL

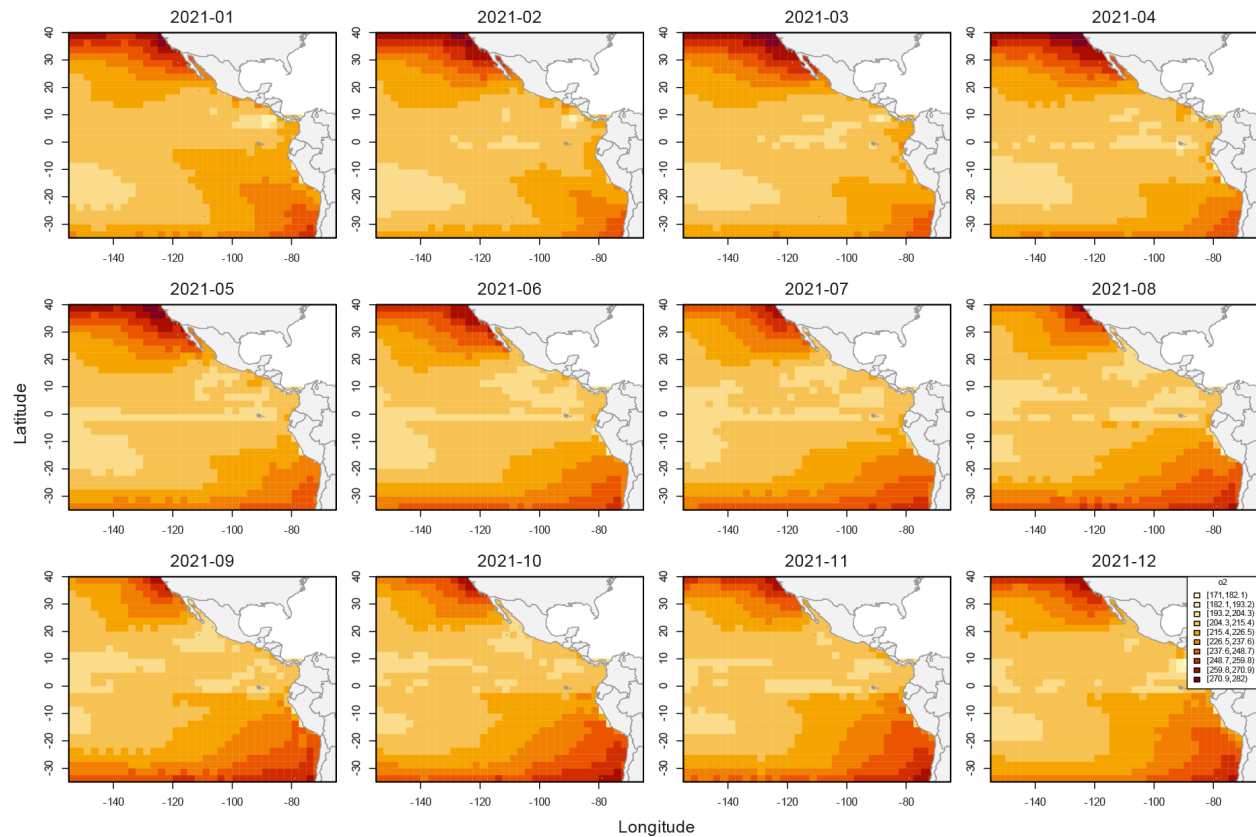


FIGURE S1: Average monthly mole concentration of dissolved molecular oxygen in sea water in upper 10m in 2021.

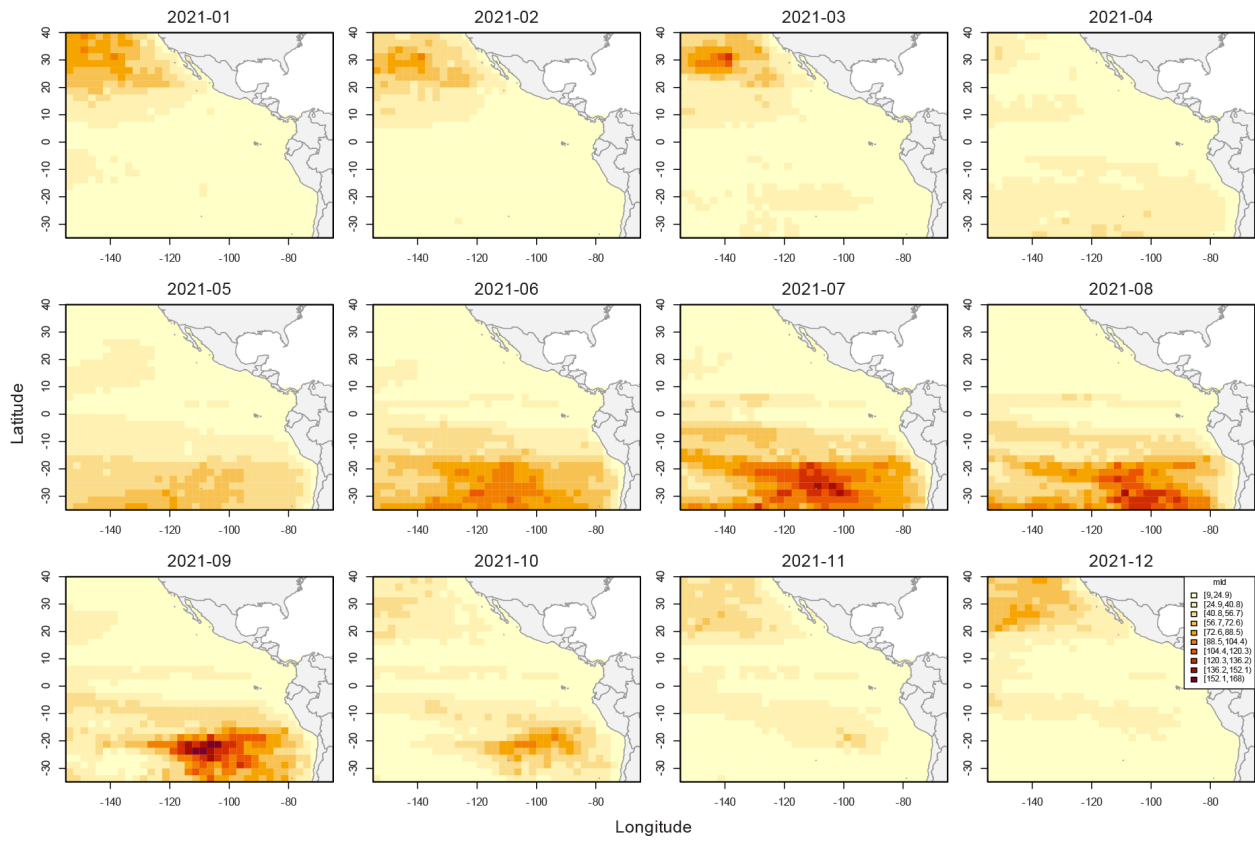
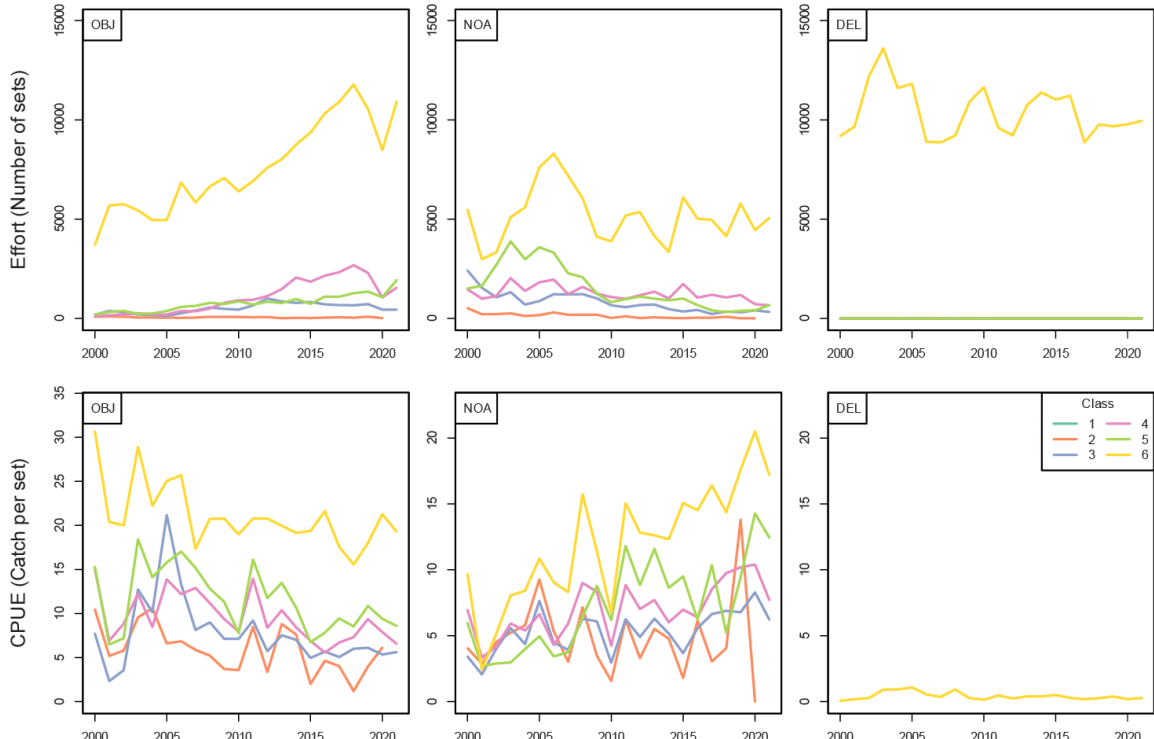


FIGURE S2: Average monthly mixed layer depth in meters in 2021.



FIGURE

FIGURE S3: Effort (number of sets) and catch per unit of effort (CPUE; catch in tons per set) for the three fleets (set-types): OBJ, NOA, and DEL, and 6 classes defining the vessel size (colored lines).

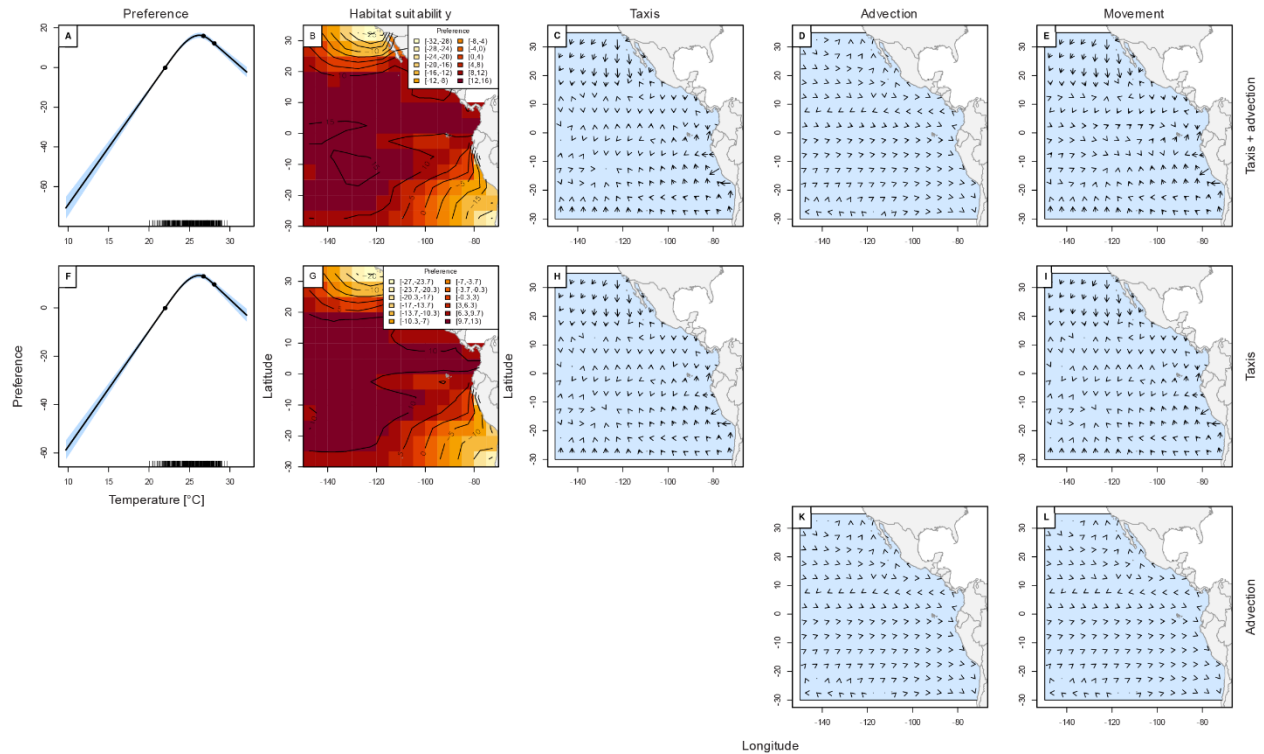


FIGURE S4: Preference function, habitat suitability, and movement rates (taxis, advection, and overall movement) for the three models with advection and taxis, only taxis, and only advection (rows).

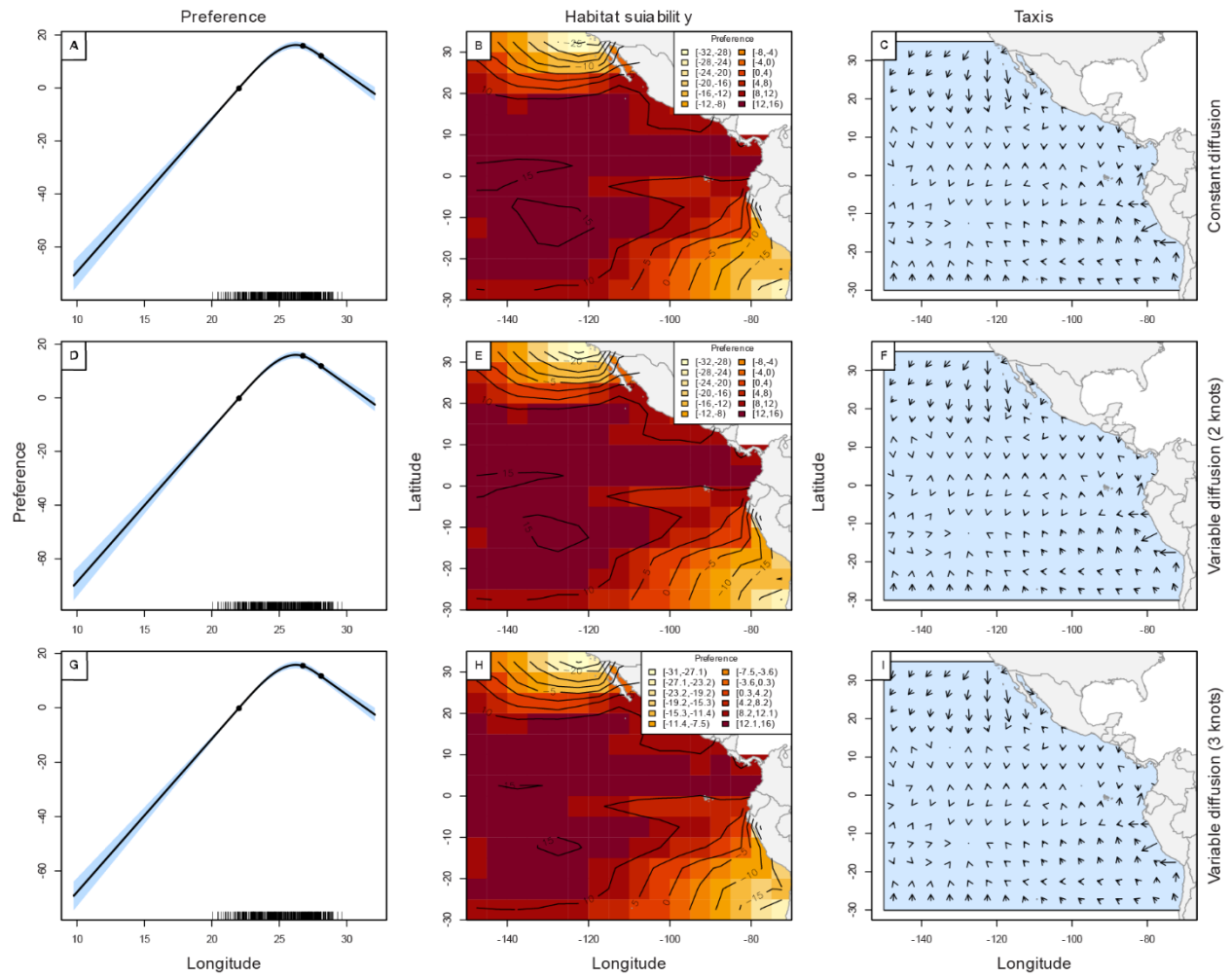


FIGURE S5: Preference function, habitat suitability, and taxis for the three models with different diffusion assumptions (constant diffusion, spline with two knots, and spline with three knots).

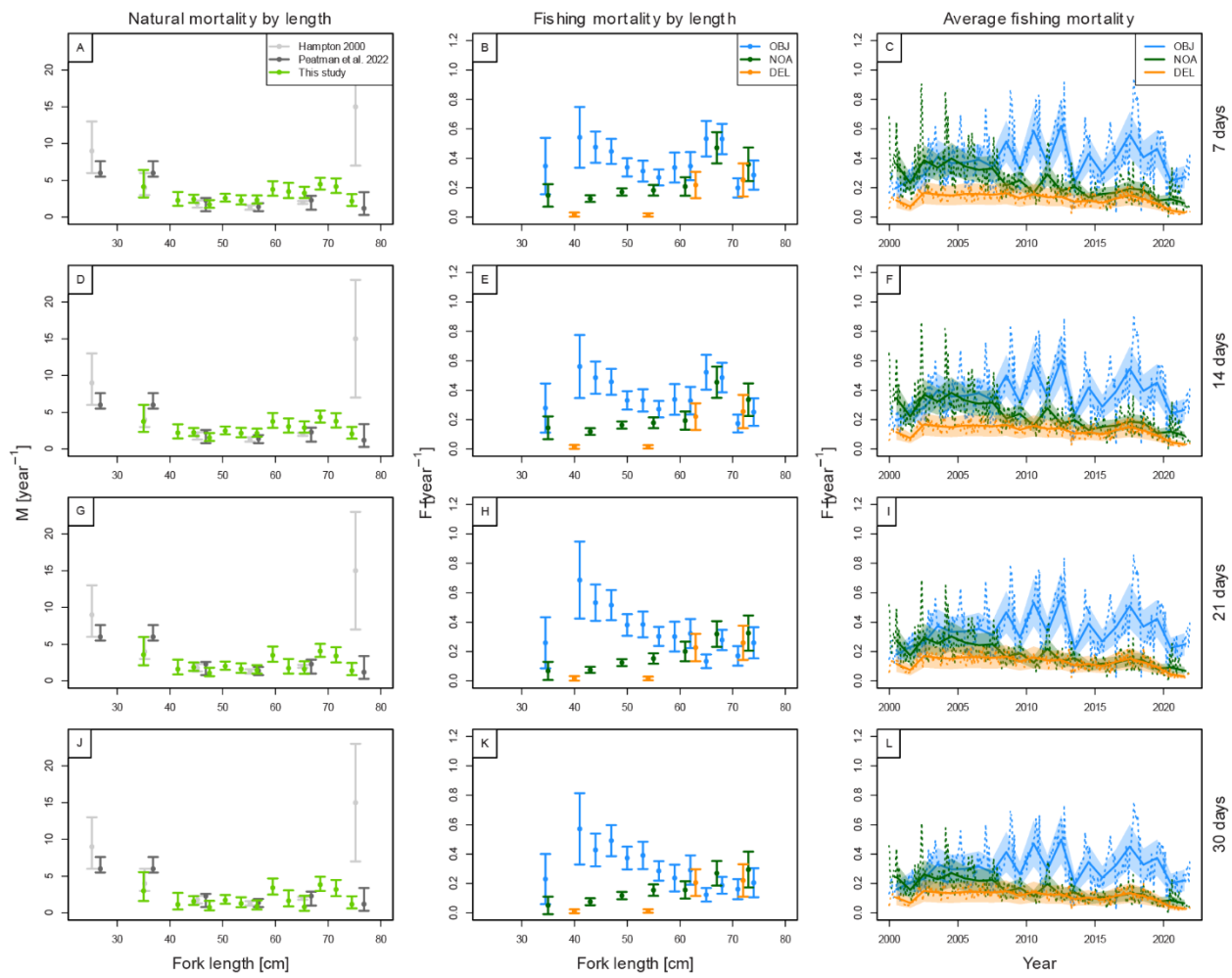


FIGURE S6: Natural mortality by length (first column), fishing mortality by length (second column), and fishing mortality over time (third column) for four models using the raw fishing effort (first row), excluding all tags recovered before X days after release, where X is between 7 and 30 days (rows).